Commun. Theor. Phys. **68** (2017) 103–110 Vol. 68, No. 1, July 1, 2017

Hydromagnetic Blood Flow of Sisko Fluid in a Non-uniform Channel Induced by Peristaltic Wave

A. Zeeshan,[1] M. M. Bhatti,[2] N. S. Akbar,[3,*] and Y. Sajjad[4]

[1]Department of Mathematics and Statistics FBAS IIUI, Islamabad, Pakistan

[2]Shanghai Institute of Applied Mathematics and Mechanics, Shanghai University, Shanghai 200444, China

[3]DBS &H CEME, National University of Sciences and Technology, Islamabad, Pakistan

[4]Government Boys Degree College, Afzalpur, Mirpur, Azad Kashmir, Pakistan

(Received January 25, 2017; revised manuscript received February 21, 2017)

Abstract *In this paper, a smooth repetitive oscillating wave traveling down the elastic walls of a non-uniform two-dimensional channels is considered. It is assumed that the fluid is electrically conducting and a uniform magnetic field is perpendicular to flow. The Sisko fluid is grease thick non-Newtonian fluid can be considered equivalent to blood. Taking long wavelength and low Reynolds number, the equations are reduced. The analytical solution of the emerging non-linear differential equation is obtained by employing Homotopy Perturbation Method (HPM). The outcomes for dimensionless flow rate and dimensionless pressure rise have been computed numerically with respect to sundry concerning parameters amplitude ratio ϕ, Hartmann number M, and Sisko fluid parameter b_1. The behaviors for pressure rise and average friction have been discussed in details and displayed graphically. Numerical and graphical comparison of Newtonian and non-Newtonian has also been evaluated for velocity and pressure rise. It is observed that the magnitude of pressure rise is maximum in the middle of the channel whereas for higher values of fluid parameter it increases. Further, it is also found that the velocity profile shows converse behavior along the walls of the channel against multiple values of fluid parameter.*

PACS numbers: 47.50.-d **DOI:** 10.1088/0253-6102/68/1/103
Key words: blood flow, peristaltic flow, Sisko fluid, non-uniform channel

1 Introduction

Peristaltic pumping is a form of fluid transport that occurs due to progressive wave generated by contraction or expansion of area along the length of distensible duct or vessel containing fluid. Most of the time, it is found in the gastrointestinal, urinary, reproductive tracts and many other glandular ducts in a living body. The functioning of heart-lung machine, blood pump machine and dialysis machine involves peristalsis mechanism. Fung and Yih presented a theoretical analysis of peristaltic transport primarily with inertia-free Newtonian flows driven by sinusoidal transverse waves of small amplitude. Investigation of peristaltic motion in connection with functions of different physiological systems such as the ureter, the gastrointestinal tract, the small blood vessels and other glandular ducts was first made by Shapiro *et al.*[2] Misra and Maiti[3] explored the peristaltic pumping of blood through small vessels of varying cross-section. Shaaban and Abou-zeid[4] studied the effects of heat and mass transfer on MHD peristaltic flow of a non-Newtonian fluid through a porous medium between two coaxial cylinders. Das[5] considered the slip effects on heat transfer and peristaltic pumping of a Johnson–Segalman fluid in an inclined asymmetric channel. Riaz *et al.*[6] found the exact solution for peristaltic flow of Jeffrey fluid model in a three-dimensional rectangular duct with wall slip. Ellahi *et al.*[7] studied the effects of heat and mass transfer on peristaltic flow in a non-uniform rectangular duct. A non-Newtonian Carreau fluid is used in this analysis. Mahmood and Fetecau[8] looked at the effects of radiative heat transfer of a Sisko fluid due to peristaltic wave in an asymmetric channel. They assumed non-uniform wall temperatures. The nonlinear equations are linearized using lubrication theory and perturbation solutions are obtained about the Sisko fluid parameter. Shafie *et al.*[9] looked at thermal diffusion and diffusion thermo effects on peristaltic flow of Sisko fluid in non-uniform channel with dissipative heating. A number of analytical and experimental studies have been reported over the years.[10−16]

Most of the theoretical and experimental investigations show that various biological fluids including blood behave like a non-Newtonian fluid. However, this present investigation is also very helpful in understanding the peristaltic flow mechanism in arteries, veins, intestine, lymphatic vessels and transfer of spermatozoa in the cervical canal. Blood performs various types of functions which include

*Corresponding author, E-mail: noreensherl@gmail.com

movement throughout the body, immune defense against various bodies and regulation of equilibria. Magnetohydrodynamics is the observation of magnetic properties of electrically conducting fluids such as plasmas, liquid metals, and salt water or electrolytes. In various physiological fluids, Magnetohydrodynamics is analyzed as fluid pump that generates continues non-pulsating flow in different microchannel designs and also very helpful in the procedure of continuous casting in metals to suppress instabilities and control the flow. In biomedical engineering, magnetohydrodynamics is very help to deliver the medicine in affected areas in cancer disease.

The study of MHD flows driven by peristaltic wave has received a great attention during the past few years due to its extensive application in various fields of biomedical sciences, such as cancer treatment, causing hyperthermia or magnetic wound, bleeding reduction during surgeries, targeted transport of drugs with the help of magnetic particles as drug carriers and magnetic resonance imagining to diagnose the disease. Kolin[17] was the pioneer who introduced electromagnetic fields in medical research and discussed the possibility of regulating the movement of blood in human system by applying magnetic field. Bengal[18] analyzed the effects of a magnetic field on blood flow flowing through an indented tube in the presence of erythrocytes. Parkash *et al.*[19] Studied MHD blood flow with heat source through bifurcated arteries. A mathematical model for biomagnetic fluid dynamics, suitable for the description of the Newtonian blood flow under the action of an applied magnetic field has been proposed by Tzirtzilakis.[20] Ikbal *et al.*[21] made a valuable discussion on unsteady response of non-Newtonian blood flow through a stenosed artery in magnetic field.

Most of the theoretical investigations regarding the blood and other physiological fluids are assumed to behave like a Newtonian fluid. Under certain situations this approach is satisfactory such as flow in ureter etc., but it fails to give an appropriate approximation for flow behavior involved in small blood vessels, lymphatic vessels, intestine, male reproductive tract and in transport of spermatozoa. It is widely acceptable that most of the physiological fluids shows a non-Newtonian nature. Blood is constantly in motion through arteries to the different organs and cells of the body. It turns back to heart by the veins. Veins are squeezed when muscles in the body contract and push the blood back to the heart. It behaves as a magnetic fluid, due to the complex interaction of the intercellular protein, cell membrane and hemoglobin as a form of iron oxides which is present at a uniquely high concentration in the mature red blood cells. Only a few recent studies[22−26] have considered this aspect of the problem. Srivastava *et al.*[27] have studied peristaltic transport of Newtonian and non-Newtonian fluid in non-uniform geometries. Mekheimer[28] investigated the peristaltic transport of couple stress blood flow through a non-uniform channel with perpendicular magnetic field. Further literature can be viewed through Refs. [29–33].

Keeping literature review in mind, this present study is to describe the effects of magnetic field on peristaltic transport of blood through a non-uniform channel. The blood here is assumed non-Newtonian in nature. The governing equations are modeled under the assumptions of long wavelength and low Reynolds number approximation. The reduced partial differential equations are solved with the help of Homotopy Perturbation Method (HPM). The graphical results of pressure rise and frictional force is discussed in reference with Hartmann number and flow rate. Observation are discussed and analyzed. The present analysis has been motivated by the fact that hydromagnetic flow of bio-fluid having properties such as Sisko fluid is very useful due to its application to physiological and engineering problems.

2 Formulation of the Problem

An incompressible and electrically conducting Sisko fluid, under the influence of uniform magnetic field is considered in a two-dimensional channel. It is also assumed that the channel is non-uniform and has electrically insulated plates with an external magnetic field B_0 applied to it. A sinusoidal oscillating wave is transmitting in the direction of flow motion with velocity c as shown in Fig. 1.

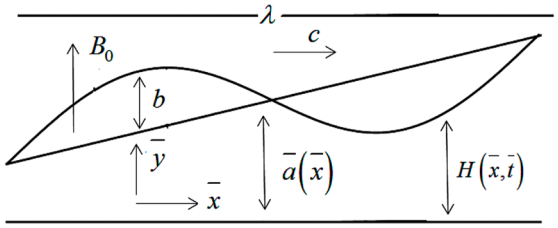

Fig. 1 Flow structure.

The velocity vector is given by

$$\bar{V} = [\bar{u}(\bar{x}, \bar{y}, \bar{t}), \bar{v}(\bar{x}, \bar{y}, \bar{t}), 0]\,. \tag{1}$$

The governing equations can be written as[33]

$$\frac{\partial \bar{u}}{\partial \bar{x}} + \frac{\partial \bar{v}}{\partial \bar{y}} = 0\,. \tag{2}$$

$\bar{x}$-component of momentum equation

$$\rho\Big(\frac{\partial \bar{u}}{\partial \bar{t}} + \bar{u}\frac{\partial \bar{u}}{\partial \bar{x}} + \bar{v}\frac{\partial \bar{u}}{\partial \bar{y}}\Big) = -\frac{\partial \bar{p}}{\partial \bar{x}} + \frac{\partial \boldsymbol{S}_{\bar{x}\bar{x}}}{\partial \bar{x}} + \frac{\partial \boldsymbol{S}_{\bar{x}\bar{y}}}{\partial \bar{y}} - \sigma B_0^2 u\,. \tag{3}$$

$\bar{y}$-component of momentum equation

$$\rho\Big(\frac{\partial \bar{v}}{\partial \bar{t}} + \bar{u}\frac{\partial \bar{v}}{\partial \bar{x}} + \bar{v}\frac{\partial \bar{v}}{\partial \bar{y}}\Big) = -\frac{\partial \bar{p}}{\partial \bar{y}} + \frac{\partial S_{\bar{y}\bar{x}}}{\partial \bar{x}} + \frac{\partial S_{\bar{y}\bar{y}}}{\partial \bar{y}}\,. \tag{4}$$

The geometry of the wall is described as

$$H(\bar{x},\bar{t}) = \overbrace{d + k\bar{x}}^{a(\bar{x})} + \bar{a}\sin 2\pi(\bar{x} - c\bar{t})\,. \tag{5}$$

The stress tensor for Sisko fluid is defined as[32]

$$\mathbf{S} = \Big[A + B\Big|\sqrt{\frac{1}{2}\mathrm{tr}(\boldsymbol{A}_1^2)}\Big|^{n-1}\Big]\boldsymbol{A}_1\,, \tag{6}$$

where

$$\boldsymbol{A}_1 = \boldsymbol{L} + \boldsymbol{L}^{\mathrm{T}}, \quad \boldsymbol{L} = \mathrm{grad}\bar{V}\,. \tag{7}$$

In Eq. (5), Sisko fluid for $n < 1$ shows shear thinning behavior, while for $n > 1$, it shows shear thickening behavior. To convert the above equations into dimensionless form, we define the dimensionless quantities as

$$\begin{aligned}
&x = \frac{\bar{x}}{\lambda}, \quad y = \frac{\bar{y}}{d^2}, \quad t = \frac{c\bar{t}}{\lambda}, \quad u = \frac{\bar{u}}{c}, \quad v = \frac{\bar{v}}{c\delta}\,,\\
&p = \frac{\bar{p}d^2}{c\lambda\mu}, \quad h = \frac{H}{d}, \quad \phi = \frac{\bar{a}}{d}\,,\\
&M^2 = B_0\bar{a}\sqrt{\frac{\sigma}{\mu}}, \quad \boldsymbol{S} = \frac{d}{\bar{a}c}\boldsymbol{S}, \quad b_1 = \frac{B}{A(a/c)^{n-1}},\\
&Re = \frac{c\rho\bar{a}}{\mu}, \quad \delta = \frac{\bar{a}}{\lambda}\,,
\end{aligned} \tag{8}$$

where $k(\ll 1)$ is a constant whose magnitude depends on the length of the channel and exit and inlet dimensions, ϕ is the amplitude ratio ($\phi < 1$), $\bar{a}$ is the wave amplitude, M is the Hartmann number, p is the pressure, $a(\bar{x})$ is the half-width of the channel at any axial distance $\bar{x}$ from inlet, λ is the wavelength, $\boldsymbol{S}$ is the stress tensor, is the viscosity of the fluid, ρ is the density, δ is the wave number, t is the time, d is the half-width at the inlet, n, A and B are the material parameters defined differently for different fluids. Note that for $B = 0$ the Newtonian fluid model is recovered and for $A = 0$ the generalized power-law model can be obtained. Using non-dimensional quantities in Eq. (1) to Eq. (6) we get,

$$\frac{\partial u}{\partial x} + \frac{\partial v}{\partial y} = 0\,, \tag{9}$$

$$\begin{aligned}
&Re\delta\Big[\frac{\partial u}{\partial t} + u\frac{\partial u}{\partial x} + v\frac{\partial u}{\partial y}\Big]\\
&\quad = -\frac{\partial p}{\partial x} + \frac{\partial \boldsymbol{S}_{xx}}{\partial x} + \frac{\partial \boldsymbol{S}_{xy}}{\partial y} - M^2 u\,,
\end{aligned} \tag{10}$$

$$\begin{aligned}
&Re\delta^3\Big[\frac{\partial v}{\partial t} + u\frac{\partial v}{\partial x} + v\frac{\partial v}{\partial y}\Big]\\
&\quad = -\frac{\partial p}{\partial y} + \frac{\partial \boldsymbol{S}_{yx}}{\partial x} + \frac{\partial \boldsymbol{S}_{yy}}{\partial y}\,,
\end{aligned} \tag{11}$$

and

$$\boldsymbol{S}_{xx} = 2\delta\Big(1 + b_1\Big|\frac{\partial u}{\partial y}\Big|^{n-1}\Big)\frac{\partial u}{\partial x}\,, \tag{12}$$

$$\boldsymbol{S}_{xy} = \boldsymbol{S}_{yx} = \Big(1 + b_1\Big|\frac{\partial u}{\partial y}\Big|^{n-1}\Big)\Big(\frac{\partial u}{\partial y} + \delta^2\frac{\partial v}{\partial x}\Big)\,, \tag{13}$$

$$\boldsymbol{S}_{yy} = 2\delta\Big(1 + b_1\Big|\frac{\partial u}{\partial y}\Big|^{n-1}\Big)\frac{\partial v}{\partial y}\,. \tag{14}$$

Here b_1 is Sisko fluid parameter. As we have the approximation of long wavelength $\delta \ll 1$ and low Reynolds number $Re \to 0$ approximation, then Eqs. (10) and (11) can be written as

$$\frac{\partial p}{\partial x} = \frac{\partial \boldsymbol{S}_{xy}}{\partial y} - M^2 u\,, \tag{15}$$

$$\frac{\partial p}{\partial y} = 0\,, \tag{16}$$

which shows that p is not a function of y. By putting the values of $\boldsymbol{S}_{xy}$, we rewrite Eq. (15) as

$$\frac{\partial p}{\partial x} = \frac{\partial}{\partial y}\Big(\frac{\partial u}{\partial y} + b_1\Big|\frac{\partial u}{\partial y}\Big|^n\Big) - M^2 u\,, \tag{17}$$

and their respective boundary conditions are

$$\frac{\partial u(0)}{\partial y} = 0, \quad u(h) = 0\,, \tag{18}$$

where

$$h = 1 + \frac{\lambda x k}{\bar{a}} + \phi\sin 2\pi(x - t)\,. \tag{19}$$

3 Solution of the Problem

To solve the overhead non-linear differential equation, the Homotopy perturbation method by He[29] is used for Eq. (17). Many scientists successfully applied this method for similar problems.[30–31] The Homotopy deformation is defined as[32–33]

$$\tilde{H}(u,m) = (1-m)(L(u) - L(u_0)) + m\Big[L(u) - \frac{\mathrm{d}p}{\mathrm{d}x} + nb_1\Big|\frac{\partial u}{\partial y}\Big|^{n-1}\frac{\partial^2 u}{\partial y^2}\Big]\,, \tag{20}$$

where m is embedding parameter i.e. $m \in [0,1]$. It can also be written as

$$\tilde{H}(u,m) = L(u) - L(u_0) + mL(u_0) + m\Big[nb_1\Big|\frac{\partial u}{\partial y}\Big|^{n-1}\frac{\partial^2 u}{\partial y^2} - \frac{\mathrm{d}p}{\mathrm{d}x}\Big]\,, \tag{21}$$

while considering a linear operator $\partial^2/\partial y^2 - M^2$, an initial guess is being taken as

$$u_0 = \frac{\cosh My}{\cosh Mh} - 1\,, \tag{22}$$

satisfies the boundary conditions

$$\frac{\partial u(0)}{\partial y} = 0, \quad u(h) = 0\,. \tag{23}$$

Let us define the expansion

$$u = u_0 + mu_1 + m^2 u_2 \cdots \tag{24}$$

By applying the linear operator L and comparing the coefficients of m, we get the following equation

$$\frac{\partial^2 u_1}{\partial y^2} - M^2 u_1 + \frac{\partial^2 u_0}{\partial y^2} - M^2 u_0 - \frac{\mathrm{d}p}{\mathrm{d}x} + n b_1 \Big|\frac{\partial u_0}{\partial y}\Big|^{n-1} \frac{\partial^2 u_0}{\partial y^2}\,, \tag{25}$$

and applying the following boundary conditions

$$\frac{\partial u_1(0)}{\partial y} = 0, \quad u_1(h) = 0\,. \tag{26}$$

We get the solution of u_1 for $n = 2$, which describes the shear thickening effect of non-Newtonian fluid model as

$$\begin{aligned} u_1 = {} & \frac{1}{(1+\mathrm{e}^{2hM})M^2}\Big[\frac{\mathrm{e}^{-M(h+2y)}}{\cosh^2 Mh}(\mathrm{e}^{hM} - \mathrm{e}^{My})\Big\{b_1(1+\mathrm{e}^{2hM} + \mathrm{e}^{2yM} + \mathrm{e}^{hM+My} + \mathrm{e}^{3hM+3My} - 4\,\mathrm{e}^{2hM+My} \\ & + \mathrm{e}^{3hM+My} - 4\,\mathrm{e}^{hM+2My} + -4\,\mathrm{e}^{hM+3My})M^3 + 6\,\mathrm{e}^{M(h+y)}(-1+\mathrm{e}^{M(h+y)})\Big(M^2 - \frac{\partial p}{\partial x}\Big)\cosh Mh\Big\}\Big]\,. \end{aligned} \tag{27}$$

Using the same iterative method we get the solution for u_2

$$\begin{aligned} u_2 = {} & \frac{-b_1\,\mathrm{e}^{M(h-3y)}}{9(1+\mathrm{e}^{2hM})^5 M}[-9b_1\,\mathrm{e}^{2hM}M^3 - 18b_1\,\mathrm{e}^{4hM}M^3 - 9b_1\,\mathrm{e}^{6hM}M^3 - 9b_1\,\mathrm{e}^{4M(h+y)}M^3 \\ & + 32b_1\,\mathrm{e}^{4hM+4My}M^3 + 32b_1\,\mathrm{e}^{M(6h+y)}M^3 - 9b_1\,\mathrm{e}^{2M(h+3y)}M^3 + 32b_1\,\mathrm{e}^{2hM+5My}M^3 \\ & + 32b_1\,\mathrm{e}^{4hM+5My}M^3 - 18b_1\,\mathrm{e}^{4hM+6My}M^3 + \mathrm{e}^{4M(2h+y)}(M^2(12+b_1M) - 12\mathrm{d}p/\mathrm{d}x) \\ & + \mathrm{e}^{2M(4h+y)}(M^2(12+b_1M) - 12\mathrm{d}p/\mathrm{d}x) + 4\,\mathrm{e}^{M(3h+y)}(M^2(9+2b_1M) - 9\mathrm{d}p/\mathrm{d}x) \\ & - 4\,\mathrm{e}^{M(3h+5y)}(M^2(9+2b_1M) - 9\mathrm{d}p/\mathrm{d}x) - 32\,\mathrm{e}^{M(5h+2y)}(M^2(3+b_1M) - 3\mathrm{d}p/\mathrm{d}x) \\ & + 4\,\mathrm{e}^{M(h+y)}(M^2(3+b_1M) - 3\mathrm{d}p/\mathrm{d}x) + 16\,\mathrm{e}^{M(h+4y)}(M^2(3+2b_1M) - 3\mathrm{d}p/\mathrm{d}x) \\ & - 4\,\mathrm{e}^{M(h+5y)}(M^2(3+2b_1M) - 3\mathrm{d}p/\mathrm{d}x) + 32b_1\,\mathrm{e}^{4hM+5My}(M^2(12+b_1M) - 12\mathrm{d}p/\mathrm{d}x) \\ & - 18b_1\,\mathrm{e}^{4hM+6My}M^3 + (\mathrm{e}^{4M(2h+y)} + \mathrm{e}^{2M(4h+y)})(M^2(12+b_1M) - 12\mathrm{d}p/\mathrm{d}x) \\ & + 4(\mathrm{e}^{M(3h+y)} - 4\,\mathrm{e}^{M(3h+5y)})(M^2(9+2b_1M) - 9\mathrm{d}p/\mathrm{d}x) + (-\mathrm{e}^{M(5h+2y)} + 4\,\mathrm{e}^{M(h+y)}) \\ & \times (M^2(3+2b_1M) - 3\mathrm{d}p/\mathrm{d}x) + (16\,\mathrm{e}^{M(h+4y)} + 4\,\mathrm{e}^{M(h+5y)})(M^2(3+2b_1M) - 3\mathrm{d}p/\mathrm{d}x) \\ & - (16\,\mathrm{e}^{M(3h+2y)} - 32\,\mathrm{e}^{M(3h+4y)})(M^2(3+2b_1M) - 3\mathrm{d}p/\mathrm{d}x) + (M^2(3+2b_1M) - 3\mathrm{d}p/\mathrm{d}x) \\ & \times (4\,\mathrm{e}^{M(7h+y)} - 16\,\mathrm{e}^{M(7h+2y)}) - (4\,\mathrm{e}^{M(7h+5y)} - 16\,\mathrm{e}^{M(5h+4y)})(M^2(3+4b_1M) - 3\mathrm{d}p/\mathrm{d}x) \\ & - 4(\mathrm{e}^{5M(h+y)} - \mathrm{e}^{M(5h+y)})(M^2(9+2b_1M) - 9\mathrm{d}p/\mathrm{d}x) - (M^2(12+b_1M) - 12\mathrm{d}p/\mathrm{d}x) \\ & \times (\mathrm{e}^{2My} - \mathrm{e}^{4My}) + 8b_1\,\mathrm{e}^{4M(h+y)}M^3(10+3My) + 8b_1\,\mathrm{e}^{2M(2h+y)}M^3(10-3My) \\ & + (-3\,\mathrm{e}^{6hM+4My} + 32\,\mathrm{e}^{2M(h+y)})(8\mathrm{d}p/\mathrm{d}x + M^2(-8 + b_1(-3+4hM-4My))) \\ & + (\mathrm{e}^{2M(h+2y)} - \mathrm{e}^{2M(3h+y)})(24\mathrm{d}p/\mathrm{d}x + M^2(-24 + b_1M(-55+12M(h+y))))]\,. \end{aligned} \tag{28}$$

By using the property of the Homotopy perturbation method, the original solution can be obtained by using

$$u = \lim_{m\to 1}(u_0 + mu_1 + m^2u_2\cdots)\,. \tag{29}$$

The first two terms of Homotopy perturbation method are written as

$$u = u_0 + u_1 + u_2\cdots \tag{30}$$

The solution for velocity profile can be written as

$$\begin{aligned} u = {} & \Big[\frac{\mathrm{e}^{-M(h+2y)}}{\cosh^2 Mh}(\mathrm{e}^{hM} - \mathrm{e}^{My})\Big\{b_1(1+\mathrm{e}^{2hM} + \mathrm{e}^{2yM} + \mathrm{e}^{hM+My} + \mathrm{e}^{3hM+3My} \\ & - 4\,\mathrm{e}^{2hM+My} + \mathrm{e}^{3hM+My} - 4\,\mathrm{e}^{hM+2My} + -4\,\mathrm{e}^{hM+3My})M^3 + 6\,\mathrm{e}^{M(h+y)}(-1+\mathrm{e}^{M(h+y)}) \\ & \times \Big(M^2 - \frac{\partial p}{\partial x}\Big)\cosh Mh\Big\}\Big]\frac{1}{(1+\mathrm{e}^{2hM})M^2} + \frac{\cosh My}{\cosh Mh} - 1 \\ & + \frac{-b_1\,\mathrm{e}^{M(h-3y)}}{9(1+\mathrm{e}^{2hM})^5 M}[-9b_1\,\mathrm{e}^{2hM}M^3 - 18b_1\,\mathrm{e}^{4hM}M^3 - 9b_1\,\mathrm{e}^{6hM}M^3 - 9b_1\,\mathrm{e}^{4M(h+y)}M^3 \\ & + 32b_1\,\mathrm{e}^{4hM+4My}M^3 + 32b_1\,\mathrm{e}^{M(6h+y)}M^3 - 9b_1\,\mathrm{e}^{2M(h+3y)}M^3 + 32b_1\,\mathrm{e}^{2hM+5My}M^3 \\ & + 32b_1\,\mathrm{e}^{4hM+5My}M^3 - 18b_1\,\mathrm{e}^{4hM+6My}M^3 + \mathrm{e}^{4M(2h+y)}(M^2(12+b_1M) - 12\mathrm{d}p/\mathrm{d}x) \\ & + \mathrm{e}^{2M(4h+y)}(M^2(12+b_1M) - 12\mathrm{d}p/\mathrm{d}x) + 4\,\mathrm{e}^{M(3h+y)}(M^2(9+2b_1M) - 9\mathrm{d}p/\mathrm{d}x) \end{aligned}$$

$$
\begin{aligned}
&- 4\,\mathrm{e}^{M(3h+5y)}(M^2(9+2b_1M)-9\mathrm{d}p/\mathrm{d}x) - 32\,\mathrm{e}^{M(5h+2y)}(M^2(3+b_1M)-3\mathrm{d}p/\mathrm{d}x)\\
&+ 4\,\mathrm{e}^{M(h+y)}(M^2(3+b_1M)-3\mathrm{d}p/\mathrm{d}x) + 16\,\mathrm{e}^{M(h+4y)}(M^2(3+2b_1M)-3\mathrm{d}p/\mathrm{d}x)\\
&- 4\,\mathrm{e}^{M(h+5y)}(M^2(3+2b_1M)-3\mathrm{d}p/\mathrm{d}x) + 32b_1\,\mathrm{e}^{4hM+5My}(M^2(12+b_1M)-12\mathrm{d}p/\mathrm{d}x)\\
&- 18b_1\,\mathrm{e}^{4hM+6My}M^3 + (\,\mathrm{e}^{4M(2h+y)} + \,\mathrm{e}^{2M(4h+y)})(M^2(12+b_1M)-12\mathrm{d}p/\mathrm{d}x)\\
&+ 4(\,\mathrm{e}^{M(3h+y)} - 4\,\mathrm{e}^{M(3h+5y)})(M^2(9+2b_1M)-9\mathrm{d}p/\mathrm{d}x) + (-\,\mathrm{e}^{M(5h+2y)} + 4\,\mathrm{e}^{M(h+y)})\\
&\times (M^2(3+2b_1M)-3\mathrm{d}p/\mathrm{d}x) + (16\,\mathrm{e}^{M(h+4y)} + 4\,\mathrm{e}^{M(h+5y)})(M^2(3+2b_1M)-3\mathrm{d}p/\mathrm{d}x)\\
&- (16\,\mathrm{e}^{M(3h+2y)} - 32\,\mathrm{e}^{M(3h+4y)})(M^2(3+2b_1M)-3\mathrm{d}p/\mathrm{d}x) + (M^2(3+2b_1M)-3\mathrm{d}p/\mathrm{d}x)\\
&\times (4\,\mathrm{e}^{M(7h+y)} - 16\,\mathrm{e}^{M(7h+2y)}) - (4\,\mathrm{e}^{M(7h+5y)} - 16\,\mathrm{e}^{M(5h+4y)})(M^2(3+4b_1M)-3\mathrm{d}p/\mathrm{d}x)\\
&- 4(\,\mathrm{e}^{5M(h+y)} - \,\mathrm{e}^{M(5h+y)})(M^2(9+2b_1M)-9\mathrm{d}p/\mathrm{d}x) - (M^2(12+b_1M)-12\mathrm{d}p/\mathrm{d}x)\\
&\times (\,\mathrm{e}^{2My} - \,\mathrm{e}^{4My}) + 8b_1\,\mathrm{e}^{4M(h+y)}M^3(10+3My) + 8b_1\,\mathrm{e}^{2M(2h+y)}M^3(10-3My)\\
&+ (-3\,\mathrm{e}^{6hM+4My} + 32\,\mathrm{e}^{2M(h+y)})(8\mathrm{d}p/\mathrm{d}x + M^2(-8+b_1(-3+4hM-4My)))\\
&+ (\,\mathrm{e}^{2M(h+2y)} - \,\mathrm{e}^{2M(3h+y)})(24\mathrm{d}p/\mathrm{d}x + M^2(-24+b_1M(-55+12M(h+y))))\Big]\,. \qquad (31)
\end{aligned}
$$

To find the instantaneous volume rates $Q(x,t)$, we define

$$Q = \int_0^{h(x)} u\,\mathrm{d}y. \qquad (32)$$

Solving Eq. (32) for the value of pressure gradient $\mathrm{d}p/\mathrm{d}x$, we have

$$
\begin{aligned}
\frac{\mathrm{d}p}{\mathrm{d}x} = {} & M^3(3b_1 + 9Q - 9b_1\mathrm{sech}^2Mh + 6b_1\mathrm{sech}^3Mh + 3b_1^2hM^3\mathrm{sech}^4Mh\\
& + 2b_1^2M\tanh hM + 3b_1^2M\mathrm{sech}^2Mh\tanh Mh - 16b_1^2M\mathrm{sech}^3Mh\tanh Mh\\
& + 8b_1^2M\mathrm{sech}^4Mh\tanh Mh)/3(2b_1^2M - 3hM - 6b_1M\mathrm{sech}^2Mh + 4b_1M\mathrm{sech}^3Mh3\tanh Mh)\,. \qquad (33)
\end{aligned}
$$

At the walls of non-uniform channel of length L, we describe the pressure rise and friction force in dimensionless form as

$$\Delta P_L(t) = \int_0^{L/\lambda} \frac{\mathrm{d}p}{\mathrm{d}x}\mathrm{d}x\,, \qquad (34)$$

$$\Delta F_L(t) = \int_0^{L/\lambda} \Big(-h\frac{\mathrm{d}p}{\mathrm{d}x}\Big)\mathrm{d}x\,. \qquad (35)$$

Special Case The result for Newtonian fluid can be obtained by taking $b_1 = 0$ in Eq. (31), we get

$$u(y) = -1 + \frac{\cosh My}{\cosh Mh} + \frac{\mathrm{e}^{M(h+y)-M(h+2y)}(\,\mathrm{e}^{hM} - \,\mathrm{e}^{My})(-1+\,\mathrm{e}^{M(h+y)})(M^2 - \partial p/\partial x)}{(1+\,\mathrm{e}^{2hM})M^2}\,. \qquad (36)$$

4 Results and Discussion

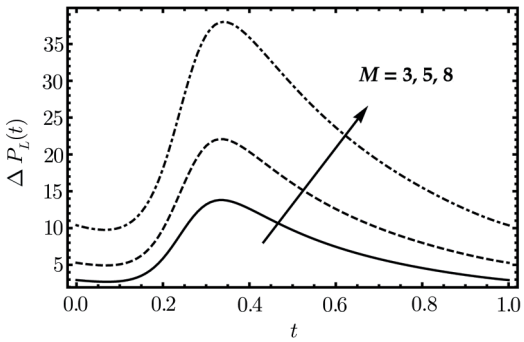

Fig. 2 Variation of pressure rise over the length of a non-uniform channel at $b_1 = 0.1$, $\phi = 0.7$, $\bar{Q} = 0$ for different values of M.

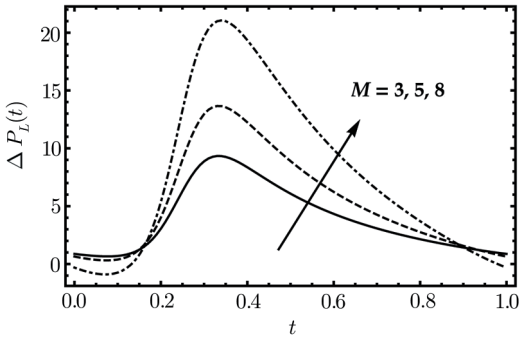

Fig. 3 Variation of pressure rise over the length of a non-uniform channel at $b_1 = 0.1$, $\phi = 0.7$, $\bar{Q} = 0.15$ for different values of M.

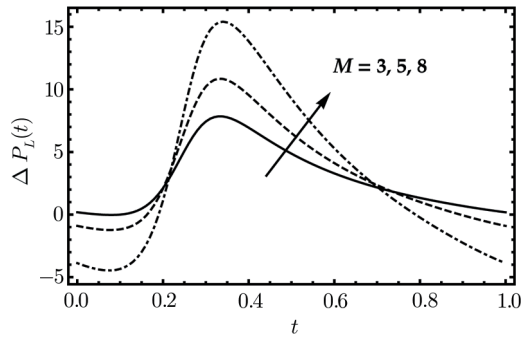

Fig. 4 Variation of pressure rise over the length of a non-uniform channel at $b_1 = 0.1$, $\phi = 0.7$, $\bar{Q} = 0.2$ for different values of M.

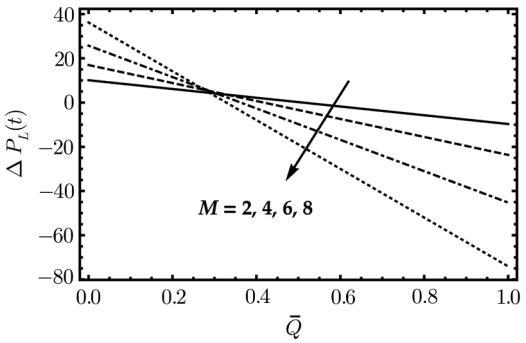

Fig. 5 Pressure versus flow rates for a non-uniform channel at $b_1 = 0.1$, $\phi = 0.7$ for different values of M.

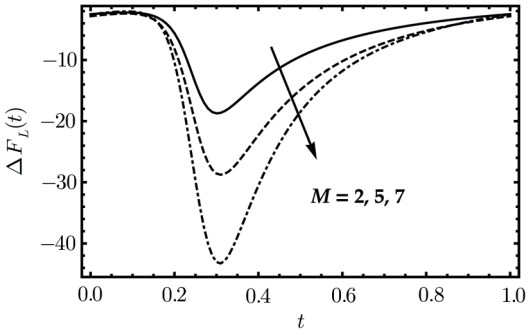

Fig. 6 Variation of friction forces over the length of a non-uniform channel at $b_1 = 0.1$, $\phi = 0.9$, $\bar{Q} = 0$ for different values of M.

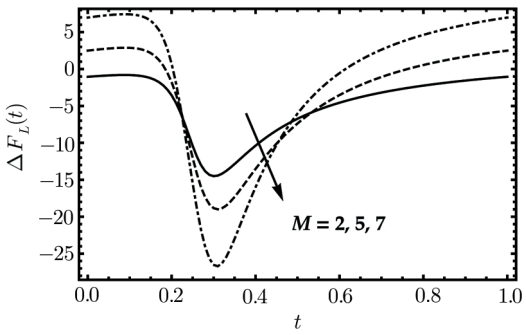

Fig. 7 Variation of friction forces over the length of a non-uniform channel at $b_1 = 0.1$, $\phi = 0.9$, $\bar{Q} = 0.15$ for different values of M.

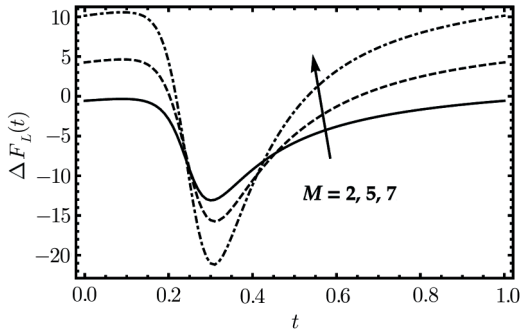

Fig. 8 Variation of friction forces over the length of a non-uniform channel at $b_1 = 0.1$, $\phi = 0.7$, $\bar{Q} = 0.2$ for different values of M.

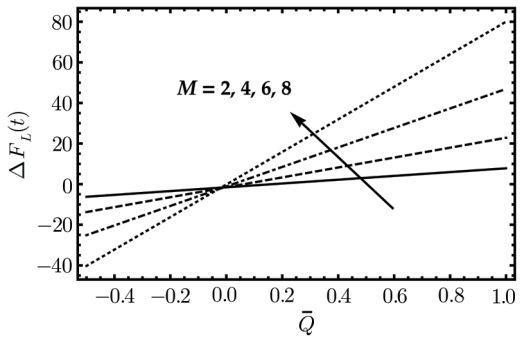

Fig. 9 Friction forces versus flow rate for a non-uniform channel at $b_1 = 0.1$, $\phi = 0.7$, $\bar{Q} = 0$ for different values of M.

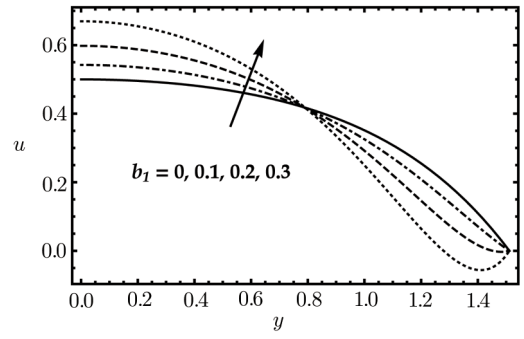

Fig. 10 Comparison of velocity profile for Newtonian and non-Newtonian fluid.

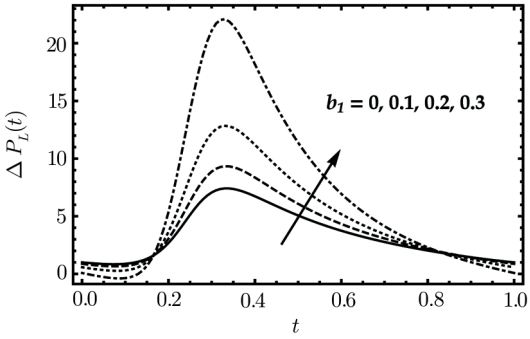

Fig. 11 Comparison of Pressure rise for Newtonian and non-Newtonian fluid.

In this section, graphical results are discussed for the value of non-dimensional pressure rise ΔP_L and frictional force ΔF_L throughout the channel for several including parameters M, ϕ and average flow rate $\bar{Q}$ over the unit time period, the average force of friction ΔF_L and pressure rise ΔP_L have been calculated. As described the values of Ref. [33] $k = 5 \times 10^{-5}$, $L = \lambda = 10$ cm and $\bar{a} = 1 \times 10^{-2}$ cm in Eqs. (34) and (35) are integrated numerically. We have considered the following form of instantaneous volume flow rate Q, which is periodic in $(x - t)$, we have

$$Q = \bar{Q} + \phi \sin 2\pi(x - t)\,, \tag{37}$$

where as $\bar{Q}$ is the average volume flow rate. Figures 2–4 display the distinction of ΔP_L with time t at $b_1 = 0.1$, $\phi = 0.7$ and for several values of M and $\bar{Q}$. From these figures it is clear that large values of M enlarge the pressure rise for smaller ΔP_L approaches to maximum at $\bar{Q} = 0$. The pressure rise drops to zero for greater values of $\bar{Q}$. Figure 5 exhibits the linear relationship between ΔP_L and $\bar{Q}$ with the parameters M. It leads us to convey that increasing values of increase the average pressure rise. Thus the measurement of ΔP_L rises for greater M, which is a straightforward evidence of the fact that the measurement of pressure rise for an MHD fluid is less than the fluid with zero magnetic field. At the end the graphical relation for the friction forces ΔF_L with M and $\bar{Q}$ is displayed in Figs. 6–9. According to these figures, it has been proved that the friction forces behave conversely as analogized to ΔP_L.

Table 1 Residual error of velocity profile (u) for Newtonian and non-Newtonian fluid.

h	Residual error for $b_1 = 0$	Residual error for $b_1 = 0.3$
0	9.176×10^{-2}	1.444×10^{-1}
0.3358	1.751×10^{-2}	6.960×10^{-2}
0.6716	7.348×10^{-3}	2.008×10^{-2}
1.0074	2.176×10^{-3}	1.948×10^{-3}
1.3432	7.798×10^{-4}	1.948×10^{-3}
1.5111	0	0

Finally, the overall conclusion can be drawn from above figures is that the Hartmann number M and flow rate have an effect on pressure rise at constant value of Sisko fluid parameter b_1. At $b_1 = 0.1$ greater values of M give greater values of pressure rise for different flow rate. The variation among the pressure rise increases for smaller values of flow rate and it approaches to maximum for zero flow rate. The friction forces show the converse actions of pressure rise. Table 1 shows the residual error of velocity profile for Newtonian and non-Newtonian fluid model. Tables 2 and 3 show the comparison for Newtonian and non-Newtonian fluid for velocity profile and pressure rise while Figs. 10 and 11 show the graphical comparison between Newtonian and non-Newtonian fluid.

Table 2 Comparison of velocity profile (u) between Newtonian and non-Newtonian fluid.

h	u for $b_1 = 0$	u for $b_1 = 0.1$	u for $b_1 = 0.2$	u for $b_1 = 0.3$
0	0.5	0.5423	0.5979	0.6696
0.1679	0.4969	0.5373	0.5906	0.6593
0.3358	0.4874	0.5221	0.5681	0.6279
0.5037	0.4703	0.4953	0.5291	0.5734
0.6716	0.4437	0.4548	0.4708	0.4925
0.8395	0.4046	0.3978	0.3905	0.3821
1.0074	0.3485	0.3214	0.2867	0.2426
1.1753	0.269	0.2243	0.1644	0.0866
1.3432	0.157	0.1106	0.0461	0.0008
1.5111	0	0	0	0

Table 3 Comparison of Pressure rise ($\Delta P_L(t)$) between Newtonian and non-Newtonian fluid.

t	$\Delta P_L(t)$ for $b_1 = 0$	$\Delta P_L(t)$ for $b_1 = 0.1$	$\Delta P_L(t)$ for $b_1 = 0.2$	$\Delta P_L(t)$ for $b_1 = 0.3$
0	1.0042	0.8730	0.5805	0.0852
0.1	0.8831	0.6947	0.3056	−0.3639
0.2	2.6836	3.0511	3.6533	5.3717
0.3	7.0648	8.8750	12.2031	21.0976
0.4	6.7354	8.3628	11.1993	18.1857
0.5	5.0706	6.0830	7.7113	11.3892
0.6	3.7475	4.3338	5.1850	6.9485
0.7	2.7704	3.0753	3.444	4.1389
0.8	2.0300	2.1434	2.2060	2.2994
0.9	1.4494	1.4257	1.2851	1.0262
1	1.0042	0.8730	0.5805	0.0852

5 Conclusion

The MHD peristaltic blood flow problem of Sisko fluid in a non-uniform channel has been investigated. The reduced governing nonlinear differential equation has been solved with the help of Homotopy Perturbation Method (HPM). The resulting solution has been obtained up to second order for velocity profile, pressure gradient, pressure rise, and friction forces. The behavior of pressure rise and friction force is discussed by varying various material parameters. The major outcomes of the present investigation are:

- The measurement of pressure rise for an MHD fluid is less than the fluid with zero magnetic field.
- The pressure rise and friction force behave conversely for sundry parameters.
- The present analysis can be reduced for Newtonian fluid by taking $b_1 = 0$.
- Numerical comparison shows that velocity of the fluid is high for non-Newtonian fluid when $y < 0.8$, however its behavior is converse for $y > 0.8$.
- Pressure rise is higher in magnitude when the fluid behaves as a non-Newtonian fluid.

References

[1] Y. C. Fung and C. S. Yih, ASME. J. Appl. Mech. **35** (1968) 669.

[2] A. H. Shapiro, M. Y. Jaffrin, and S. L. Weinberg, J. Fluid Mech. **37** (1969) 799.

[3] J. C. Misra and S. S. Maiti, ASME. J. Appl. Mech. **79** (2012) 061003.

[4] A. A. Shaaban and M. Y. Abou-zeid, Math. Probl. Eng. **2013** (2013) 1.

[5] K. Das, Arab. J. Math. **1** (2012) 159.

[6] A. Riaz, S. Nadeem, R. Ellahi, and A. Zeeshan, Appl. Bio. Biomech. **11** (2014) 81.

[7] R. Ellahi, A. Riaz, S. Nadeem, M. Ali, Math. Prob. Eng. **2012** (2012) 1.

[8] O. U. Mehmood and C. Fetecau, Appl. Biol. Biomech. **2012** (2015) 1.

[9] S. Shafie, O. U. Mehmood, and N. Mustapha, J. Heat Transf. **135** (2013) 122004.

[10] N. S. Akbar, S. Nadeem, and M. Ali, J. Mech. Med. Biol. **11** (2011) 529.

[11] R. Ellahi, M. M. Bhatti, and K. Vafai, Int. J. Heat Mass Transf. **71** (2014) 706.

[12] R. Ellahi, M. M. Bhatti, C. Fetecau, and K. Vafai, Commun. Theor. Phys. **65** (2016) 66.

[13] R. Ellahi, S. U. Rahman, S. Nadeem, and K. Vafai, Commun. Theor. Phys. **63** (2015) 353.

[14] A. Khan, S. Muhammad, R. Ellahi, and Q. Z. Zia, J. Magn. **21** (2016) 273.

[15] R. Ellahi, S. U. Rahman, and S. Nadeem, Phys. Lett. A **378** (2014) 2973.

[16] R. Ellahi, M. M. Bhatti, and I. Pop, Int. J. Numer. Method. H. **26** (2016) 1802.

[17] Kolin, Exp. Biol. Med. (Maywood) **35** (1936) 53.

[18] W. Bengal, Indian J. Pure Appi. Math. **25** (1994) 345.

[19] O. Prakash, S. P. Singh, D. Kumar, and Y. K. Dwivedi, AIP Adv. **1** (2011) 042128.

[20] E. E. Tzirtzilakis, Physica D **237** (2008) 66.

[21] M. A. Ikbal, S. Chakravarty, K. K. Wong, *et al.*, J. Comput. Appl. Math. **230** (2009) 243.

[22] S. U. Rahman, R. Ellahi, S. Nadeem, and Q. Z. Zia, J. Mol. Liq. **218** (2016) 484.

[23] G. Bohme and F. Friedrich, J. Fluid Mech. **128** (1983) 109.

[24] A. M. Siddiqui and W. H. Schwarz, J. Non-Newtonian Fluid Mech. **35** (1994) 257.

[25] R. Ellahi, E. Shivanian, S. Abbasbandy, and T. Hayat, Int. J. Numer. Method. H **26** (2016) 1433.

[26] R. Ellahi, Appl. Math. Model **37** (2013) 1451.

[27] L. M. Srivastava, V. P. Srivastava, and S. N. Sinha, Biorheology **20** (1983) 153.

[28] Kh. S. Mekheimer, Appl. Math. Comput. **153** (2004) 763.

[29] J. H. He, Phys. Lett. A **350** (2006) 87.

[30] A. Ebaid, Comput. Math. Appl. **68** (2014) 77.

[31] N. S. Akbar, S. Nadeem, T. Hayat, and A. A. Hendi, Heat Mass Trans. **48** (2012) 451.

[32] M. M. Bhatti, A. Zeeshan, and R. Ellahi, Comput. Biol. Med. **78** (2016) 29.

[33] M. A. Abbas, Y. Q. Bai, M. M. Rashidi, and M. M. Bhatti, J. Mech. Med. Biol. **16** (2016) 1650052.